Int. J. Multiphase Flow Vol. 12, No. 6, pp. 935–955, 1986
Printed in Great Britain.

0301-9322/86 $3.00 + 0.00

STRUCTURE, PHYSICAL PROPERTIES AND DYNAMICS OF MAGNETORHEOLOGICAL SUSPENSIONS

Z. P. SHULMAN, V. I. KORDONSKY, E. A. ZALTSGENDLER,
I. V. PROKHOROV, B. M. KHUSID and S. A. DEMCHUK
Luikov Heat and Mass Transfer Institute, BSSR Academy of Sciences, Minsk, U.S.S.R.

(*Received* 24 *January* 1985; *in revised form* 25 *November* 1985)

Abstract—The dynamic structure and physical properties (rheological, magnetic) of magnetorheological suspensions are described in terms of a stationary model, according to which a suspension in a magnetic field represents a system of ordered non-interacting ellipsoidal aggregates oriented at some angle to the flow. The model is verified experimentally by measurements of steady-state effective rheological and magnetic characteristics.

1. INTRODUCTION

One of the direct influences on the mechanical properties of a fluid is the magnetorheological effect (MRE). In this respect it represents a reversible change (increase), due to an external magnetic field of effective viscosity of a noncolloid suspension of magnetic particles. Such suspensions are normally called magnetorheological suspensions (MRSs) and usually structural transformations in the dynamic system dispersed medium–magnetized dispersed phase are responsible for their complicated rheological specificity (Harvey 1953; Bibik 1981; Shulman & Kordonsky 1982; Batchelor 1976). In a magnetic field other physical properties of MRSs are sensitive to a structure state; in particular, thermal and electric conductivities undergo essential changes.

Descriptions of the MRE (Shulman & Kordonsky 1982) have been presented in terms of representations conventional to the theory of the rheology of dispersed systems, according to which an increase in the suspension's viscosity is attributed to additional energy consumption for destruction of structural elements generated by the field. Since in classic theories a structural element is not identified with real physical characteristics of the system, such physical characteristics as magnetic strength and magnetic properties of a dispersed phase are introduced by considering a chain of magnetic dipoles as a structural element.

Apart from predicting the viscoplastic character of the flow these models do not allow determination of other important physical properties necessary for describing transfer processes in MRSs.

The theoretical approach described below is based, not on the structural rheology but, on the current statistical theory of suspensions that employs certain physical characteristics of a microstructure. Grounded experimentally (by MRS structure diagnostics involving simultaneous measurement of its macroscopic characteristics, i.e. the magnetic and rheological ones), a stationary model is considered, according to which a suspension represents an ordered system formed by dispersed-phase particles and oriented at some angle to the shear flow of non-interacting ellipsoidal aggregates. The increase in viscosity is due to additional energy consumption by a carrier medium passing these structural elements. The level of mechanical energy dissipation (apparent viscosity) is controlled by variation of the given MRS microstructure (elongation of aggregates and their angle of orientation), the external magnetic field strength or the shear rate. Detailed information on a dynamic microstructure is then employed for defining the main physical properties, i.e. rheological, thermophysical and magnetic, of the MRS.

2. MRSs—GENERAL COMMENTS

MRSs represent stable suspensions in a carrying fluid containing non-colloidal magnetic particles of size 10^{-4}–10^{-3} cm. For these dispersed systems, Brownian movement is of no importance. Depending upon the type and concentration of the dispersed phase, aggregative and sedimentation stability of MRSs is provided by one of the following methods.

Course-dispersed small-concentration systems are stabilized by the introduction of additives, forming a protective colloidal structure in the bulk of the carrier. The strength of this structure should be such as to prevent sedimentation and spontaneous irreversible coagulation of magnetic particles, on the one hand, and to allow reversible thyxotropic transformations and not to inhibit the system structurization in the magnetic field, on the other.

In the case of sufficiently fine dispersed concentrated suspensions this stability may be achieved by introduction of surfactants and formation of a spatial structure just from ferromagnetic particles. Stability is a necessary but still insufficient condition of the MRS's existence as an object of a hydrodynamic system. Outside the field it should possess satisfactory fluidity and recover quickly after ceasing shear flow. Some peculiarities in the mechanical properties of MRSs are brought about by the nature of the dispersed-phase material, viz. magnetosoft or magnetorigid (Shulman & Kordonsky 1982).

The experimental results below have been obtained with suspensions of carbonyl iron magnetosoft powder R-10 (multidomain spherical particles, $d_m \sim 3.5\ \mu$m), whose volumetric concentration constitutes 2, 4, 6, 8 and 10%. The hydraulic fluid AMG-10 served as a continuous medium. Gel-forming additives were introduced into the medium to ensure stability of the system.

3. MAGNETIC CHARACTERISTICS AND STRUCTURAL AND RHEOLOGICAL PROPERTIES OF MRSs (EXPERIMENT)

Interdependence between the rheological properties of the material and its structure is generally stated nowadays. In magnetic rheology a system approach has been developed, beginning with the first papers dealing with the effects of an increase in viscosity of dispersed ferromagnetics in a magnetic field (Harvey 1953; Bibik 1981).

In order to get information on a detailed MRS structure use has been made of optical and magnetic measurements electron microscopy and X-ray diffraction analysis. It has been found that an external magnetic field imposed on a magnetic suspension initiates the formation of threads (fibres, chains, aggregates etc.) from the dispersed-phase particles which are spread throughout the field. However, all these data have been referred, as a rule, to static systems at rest. Their use is of no help for a qualitative description of the complex dynamic process which represents MRS strain. As is shown below, as the shear rate increases there occurs disintegration of aggregates (chains), initially grown through the whole cross-section of the flow, in such a way that a certain set of structural elements and the definite system morphology, i.e. mutual arrangement of elements in space, correspond to each combination of the prescribed parameters (viscosity of the continuous medium, magnetic properties of the particles, magnetic strength and strain rate).

A study of the dynamic structure of MRSs encounters some difficulties. The present paper is an attempt to implement MRS microstructure diagnostics by simultaneous measurement of their macroscopic, i.e. magnetic and rheological, characteristics.

3.1. Experimental Procedure

With the aim of achieving adequate confrontation of an effective increment of MRS viscosity in a magnetic field and its magnetic characteristics for pure shear strain an experiment has been conducted according to the following scheme (figure 1).

Coaxially-cylindrical rheometric cells (1 and 2) with a bell-type rotor were placed in a radial magnetic field initiated in an annular gap of an electromagnet (3 and 4), with the latter being connected to a current source (Shulman & Kordonsky 1982). The cell elements

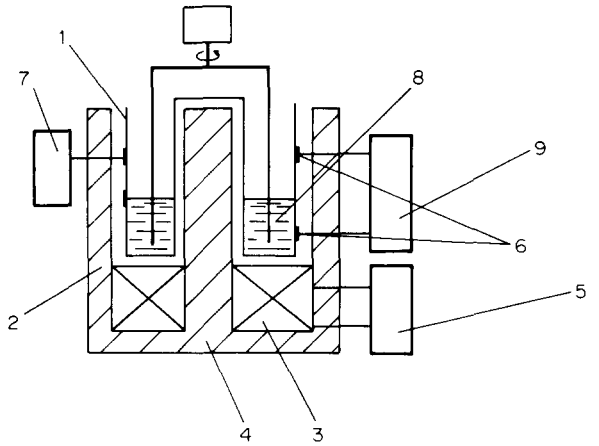

Figure 1. Schematic drawing of the experimental setup: 1, bell; 2, fixed cylinder; 3, electromagnet winding; 4, magnetic circuit; 5, current source; 6, Hall probe; 7, 9, digital induction meters; 8, MRS.

were made of non-magnetic material. On an external side of fixed cylinder 2 two miniature Hall probes (6) were mounted which were full-wave circulated in opposition and connected to digital meter 9. MRS 8 is poured into the cell so as to have its "mirror" between the Hall probes, with one of them (the lower) being in a zone of magnetic flux action across the MRS, the other (the upper) being in an air gap. The total signal at the meter is proportional only to the magnetic induction increment ΔB due to the presence of the MRS in the magnetic clearance. Meter 7 also reads the induction in the air gap. A calculation diagram of the experiment concerned with the measurement of magnetic MRS properties is presented in figure 2. At the point in the gap where there is no suspension (above the suspension level), the law of total current for a magnetic circuit is written in the form (Atabekov 1969)

$$H \cdot l = F,$$

where F is the magnetization force and H is the field in the gap above the suspension. Since $H = B/\mu_0$, then neglecting the losses in the magnetic circuit the magnetization force can be specified as

$$F = \frac{B \cdot l}{\mu_0}.$$

Here μ_0 is the magnetic constant with B being the induction in the gap above the suspension. For the part of the gap containing the suspension, the total current law is written as

$$H_h \cdot l_h + H_s \cdot l_s = F$$

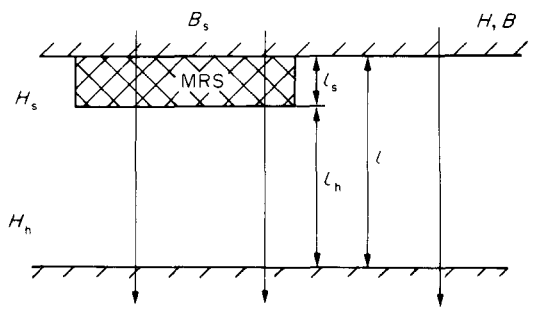

Figure 2. Calculation diagram of the experimental measurements of the MRS magnetic properties.

or in the form

$$\frac{B_s l_h}{\mu_a} - \frac{B_s l_s}{\mu_0 \mu} = \frac{B \cdot l}{\mu_0}, \qquad [1]$$

where B_s is the induction in the part of the gap containing the suspension and μ is the MRS permeability. With reference to [1] we find

$$B_s = \frac{B \cdot l}{l_h + l_s/\mu}.$$

The measured increment in the induction due to MRS loading reads

$$\Delta B = B_s - B = B \frac{1 - \frac{1}{\mu}}{\frac{l_h}{l_s} + \frac{1}{\mu}}, \qquad [2]$$

wherein l_h is the middle line length of magnetic induction of a section occupied by air at the lower probe and l_s stands for a section occupied by the MRS. With the MRS permeability μ being known, one can calculate the field in the air gap involving the suspension:

$$H_h = \frac{B_s}{\mu_0} = \frac{B}{\mu_0}\left[\frac{1}{1 + \left(\frac{1}{\mu} - 1\right)\frac{l_s}{l}}\right] \qquad [3]$$

Expression [2] allows easy evaluation of the magnetic permeability (susceptibility) of the MRS and calculation of its magnetization for each field H_B.

Rheological characteristics are determined by a conventional technique involving torque measurement on a rotating cylinder. So simultaneous measurement of the effective rheological and magnetic characteristics of an MRS subjected to shear stress is implemented.

3.2. Magnetic Characteristics and Structure of MRSs

A specific feature of an MRS as a magnetic material is the mechanical mobility of the carriers of a magnetic moment, i.e. particles of the dispersed phase. Such systems undergo magnetization to a considerable extent, due only to rearrangement (ordering) of their structure. This means that a definite structure of magnetic particles corresponds to each level of magnetization. The interdependence between the magnetic properties of an MRS and its microstructure is demonstrated well by the data presented in figure 3. A ballistic method has been employed to determine the magnetization of a model dispersed system consisting of carbonyl iron particles (10 vol%) suspended in a matrix capable of modifying its aggregative state upon heating. When the matrix is in a solved state, the particles are distributed uniformly in the bulk and do not move, i.e. magnetization is not accompanied by structurization. This situation may be treated as a model of an ultimately destroyed structure whose magnetization process is shown by curve 2 in figure 3. Curve 1 shows the magnetization of the material preheated in a strong magnetic field up to a temperature exceeding that of a phase transition and then cooled. This is the way the ultimately oriented structure has been modeled.

In the theoretical presentation of the magnetic characteristics of suspensions with a small content of magnetic particles in the bulk, consideration is given to random isolated magnetosoft particles whose mutual effect is accounted for in a dipole–dipole approximation by the Lorenz–Lorents method (Landau & Lifshits 1957; Dukhin & Shilov 1972). In this case the macroscopic characteristics are found by averaging of the macroscopic quantities with respect to the position and orientation of the particles. As applied to MRSs, of greatest interest are the ordered systems in which structural elements are oriented at

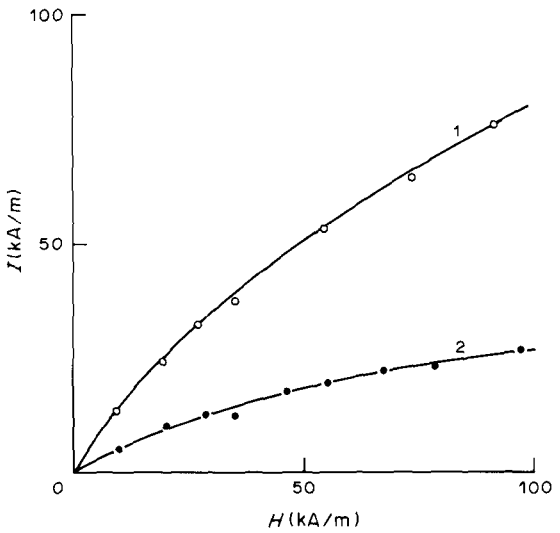

Figure 3. MRS microstructure effect on its magnetic properties: 1, MRS is oriented in the magnetic field; 2, not oriented.

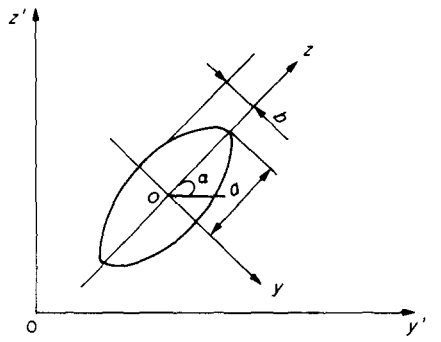

Figure 4. The ellipsoid in the magnetic field.

the same angle towards the field. In a general case, magnetization of a suspension of ellipsoidal particles (aggregated) is defined as

$$I_i = \frac{\kappa_a \mu_0}{1 + \kappa_a n_i} G_i \varphi, \qquad [4]$$

wherein I_i is the suspension magnetization along the ith axis (in a system of coordinates related to a particle); κ_a is the aggregate susceptibility, μ_0 is the magnetic constant, n_i are the demagnetizing factors along the corresponding axes, G_i are the vector components of an effective field acting on the particles and φ is the concentration of particles. For a cartesian system of coordinates in which the z-axis coincides with a long axis of an aggregate (figure 4) we have:

$$n_z = \frac{1 - e^2}{2e^3}\left(\ln\frac{1+e}{1-e} - 2e\right) \quad \text{and} \quad n_x = n_y = \tfrac{1}{2}(1 - n_z), \qquad [5a]$$

where

$$e = \sqrt{1 - r_e^{-2}} \quad \text{and} \quad r_e = \frac{a}{b}; \qquad [5b]$$

here a is the semimajor axis of an ellipsoidal aggregate and b is the semiminor axis.

The field strength in the suspension (in the system of coordinates related to a particle) reads

$$H_i = G_i\left(1 - \frac{1}{3}\frac{\kappa_a \varphi}{1 + \kappa_a n_i}\right). \qquad [6]$$

With reference to [4] and [6] we derive a formula for the susceptibility component of the suspension along the field:

$$\kappa_s = \kappa_a \varphi \frac{\dfrac{G_z \sin\alpha}{1 + \kappa_a n_z} - \dfrac{G_y \cos\alpha}{1 + \kappa_a n_y}}{G_z \sin\alpha\left[1 - \dfrac{\kappa_a \varphi}{3(1 + \kappa_a n_z)}\right] - G_y \cos\alpha\left[1 - \dfrac{\kappa_a \varphi}{3(1 + \kappa_a n_y)}\right]}, \qquad [7]$$

where α is the angle between the long particle axis and the direction perpendicular to the field and the vector components of the effective field are as follows:

$$G_y = -\frac{A_4 \cos\alpha}{A_3 A_1 \sin^2\alpha + A_2 A_4 \cos^2\alpha} H_e$$

and

$$G_z = \frac{A_3 \sin\alpha}{A_4 A_2 \cos^2\alpha + A_3 A_1 \sin^2\alpha} H_e;$$

here H_e is the external magnetic strength,

$$\left.\begin{aligned} A_1 &= 1 + \frac{\kappa_a}{1+\kappa_a n_z}\frac{2\varphi}{3}, & A_3 &= 1 - \frac{\kappa_a}{1+\kappa_a n_y}\frac{\varphi}{3}, \\ A_2 &= 1 + \frac{\kappa_a}{1+\kappa_a n_y}\frac{2\varphi}{3} \quad \text{and} & A_4 &= 1 - \frac{\kappa_a}{1+\kappa_a n_z}\frac{\varphi}{3}. \end{aligned}\right\} \quad [8]$$

The initial susceptibility of the system of uniformly volume-distributed spherical particles is determined from [7] as

$$\kappa_c = \frac{3\kappa_p\varphi}{3 + \kappa_p - 3\kappa_p\varphi}, \quad [9]$$

wherein κ_p is the initial susceptibility of a particle. The values of initial susceptibility found by this formula for the suspensions studied, particularly in the case of small concentrations, appeared to be rather close to those obtained experimentally for the destroyed structure (see table 1).

In the calculations the quantity κ_p has been assumed to be equal to 50 (Tolmassky 1976). The matter is more complicated when seeking the initial susceptibility of a structurized MRS consisting of a system of anisodiametric aggregates. For a system of elongated monolithic ellipsoidal particles this quantity may be defined by [7] as

$$\kappa_s = \frac{\kappa_a\varphi_a}{1 - \frac{\kappa_a\varphi_a}{3}} = \frac{3\kappa_a\varphi_a}{3 - \kappa_a\varphi_a}. \quad [10]$$

An aggregate formed in this field is not monolithic but consists of ferromagnetic particles positioned very close to each other. Limiting packing of spherical particles corresponds to their concentration (60–70% of the aggregate bulk). Taking into account the fact that the particles are well-wetted with the continuous medium and, therefore, possess a solvation jacket which hinders their being in close contact, the volumetric particle concentration in the aggregate amounts to 0.4–0.6. This means that the concentration of aggregates in the MRS is $\varphi_a \sim \varphi/\phi$, where ϕ indicates the degree of filling of the aggregate. On the other hand, [10] is valid only for elongated ellipsoids with a long axis/cross-section ratio $\geqslant 10$. In this case the susceptibility does not depend on ellipsoid length. The following experiments show that a chain aggregate is quite consistent with such a model. A vibromagnetometer has been used to determine the magnetization of a system assembled from a different amount of equal-sized steel balls forming a chain along the field. The balls have been in close contact or at a distance equal to their diameter. It turns out that the magnetization of such a system increases with the amount of balls and attains its limit with the total length of the sample equal to 7–8 diameters of the ball.

All this allows use of [10] for evaluating the susceptibility of oriented MRSs. The quantity κ_a, found in this way, was equal to 5 at $\phi = 0.5$. This is appropriate for the

Table 1. Initial MRS susceptibility

	Destroyed structure		Oriented structure
φ	κ_{calc}	κ_{exp}	κ_{exp}
0.1	0.394	0.47	1.1
0.08	0.292	0.35	0.9
0.06	0.204	0.24	0.62
0.04	0.127	0.15	0.47
0.2	0.06	0.09	0.25

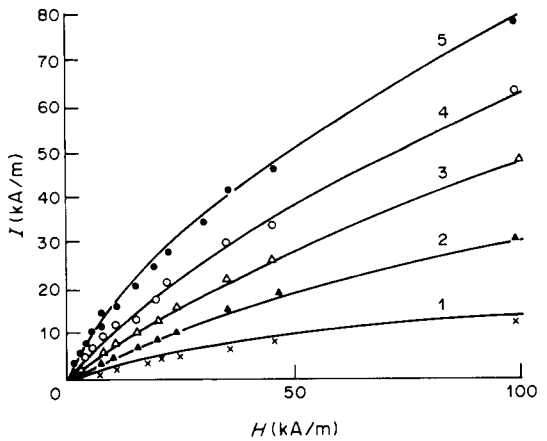

Figure 5. Magnetization curves of carbonyl iron-based MRS: 1, $\varphi = 0.02$; 2, $\varphi = 0.04$; 3, $\varphi = 0.06$; 4, $\varphi = 0.08$; 5, $\varphi = 0.1$.

susceptibility values obtained for a carbonyl iron R-10-based magnetodielectric representing a compressed ultimately concentrated system with $\varphi \sim 0.6$ (Tolmassky 1976).

Magnetization curves of all the tested (at rest) MRSs are shown in figure 5. The dotted curves indicate measurements made by the procedure described in section 3.1, while solid lines represent the data of reference tests performed on a standard ballistic magnetometric setup. Any departure from the ballistic curves was less than 10%. The data present evidence that the magnetization curves in their initial stages approach the linear ones, up to field strengths of $H = 30$ kA/m. Therefore, the materials tested in this region exhibit constant susceptibility ($\kappa_s = I/H = \text{const}$). Besides, the initial susceptibility of MRSs practically increases linearly with concentration.

Henceforth all the experiments and calculations have been conducted only for the initial susceptibility region. As follows from figure 6 the susceptibility is rather responsive to changes in the structure under shear flow. The figure presents the initial susceptibility κ_s of each tested MRS as a function of the shear rate $\dot{\gamma}$ at field strengths of $H = 24$ kA/m (——) and 35.3 kA/m (– – –), respectively. For MRSs at rest the susceptibility does not depend on the field, and in shear flow the situation is reversed: the susceptibility falls with

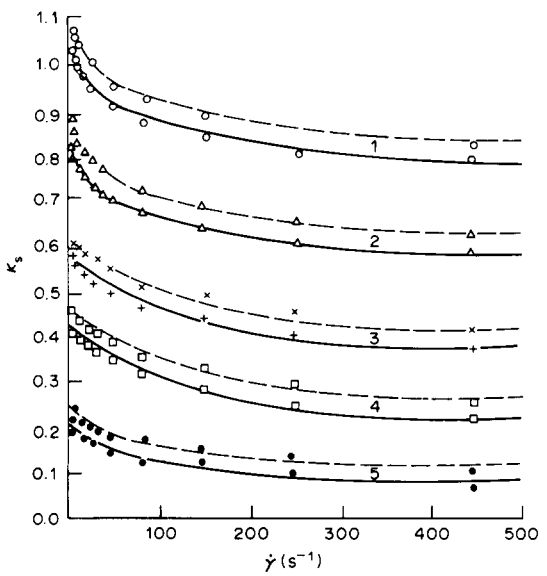

Figure 6. Initial MRS susceptibility vs shear rate: 1, $\varphi = 0.1$; 2, $\varphi = 0.08$; 3, $\varphi = 0.06$; 4, $\varphi = 0.04$; 5, $\varphi = 0.02$.

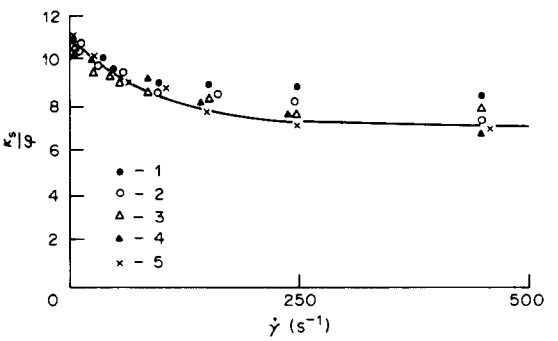

Figure 7. Reduced magnetic susceptibility vs shear rate: 1, $\varphi = 0.1$; 2, $\varphi = 0.08$; 3, $\varphi = 0.06$; 4, $\varphi = 0.04$; 5, $\varphi = 0.02$. $H = 24$ kA/m.

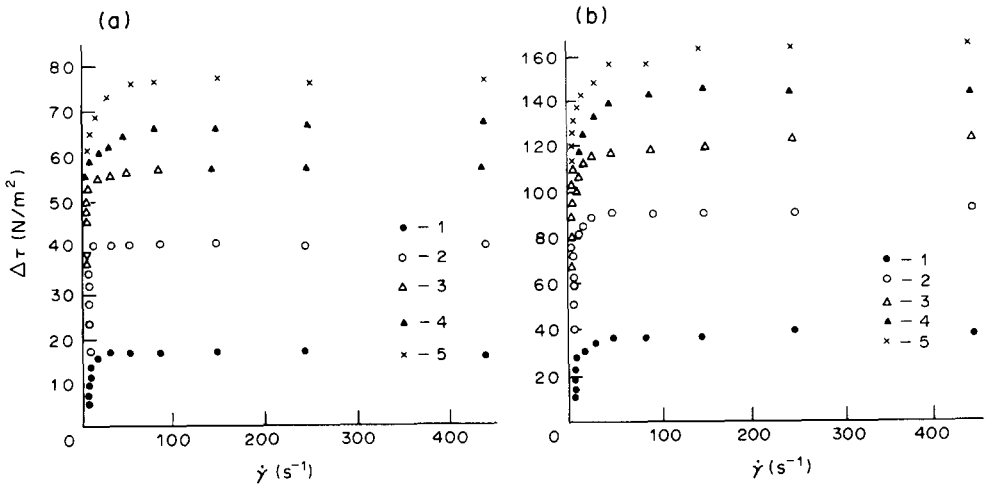

Figure 8. Shear stress increment vs shear rate, (a) $H = 24$ kA/m and (b) $H = 35.3$ kA/m: 1, $\varphi = 0.02$; 2, $\varphi = 0.04$; 3, $\varphi = 0.06$; 4, $\varphi = 0.08$; 5, $\varphi = 0.1$

shear rate and with a decrease in field strength. On the one hand, in small fields at sufficiently large shear rates the susceptibility tends to the values corresponding to a completely destroyed structure, on the other hand, a field increase at a fixed shear rate results in susceptibility enhancement. It is quite reasonable to suppose that these changes in the susceptibility are initiated by those in the aggregates' sizes or their orientation towards the field and, obviously, are specified by some relationship between the magnetic and hydrodynamic forces. The dependences $\kappa_s = \kappa_s(\dot{\gamma})$, based on concentration, are generalized at the given field strength by a single curve (figure 7) that indicates a similar type of structure changes are initiated by shear flow for all the MRSs tested.

3.3. Rheological Characteristics

In the experiments, a shear stress increment in a magnetic field $\Delta\tau = \tau_H - \tau_{H=0}$ as a function of shear rate has been determined for two magnetic field strengths (figure 8). The dependences $\Delta\tau = \Delta\tau(\dot{\gamma})$ are essentially nonlinear within a range of small shear rates. With an increase in shear rate, the quantity tends to some constant value defined only by field

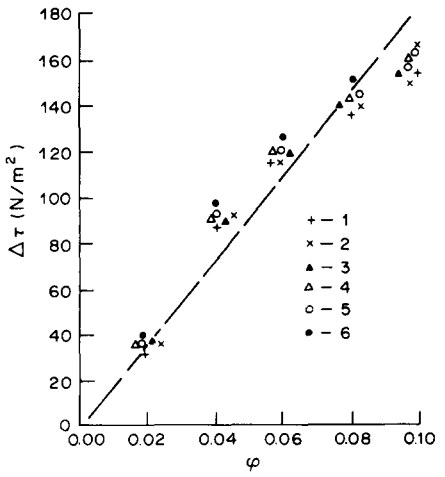

Figure 9. Shear stress increment in the magnetic field vs concentration ($H = 35.3$ kA/m): 1, $\dot{\gamma} = 27.7\ s^{-1}$; 2, $\dot{\gamma} = 39.4\ s^{-1}$; 3, $\dot{\gamma} = 82.2\ s^{-1}$; 4, $\dot{\gamma} = 146.8\ s^{-1}$; 5, $\dot{\gamma} = 256.0\ s^{-1}$; 6, $\dot{\gamma} = 444.5\ s^{-1}$.

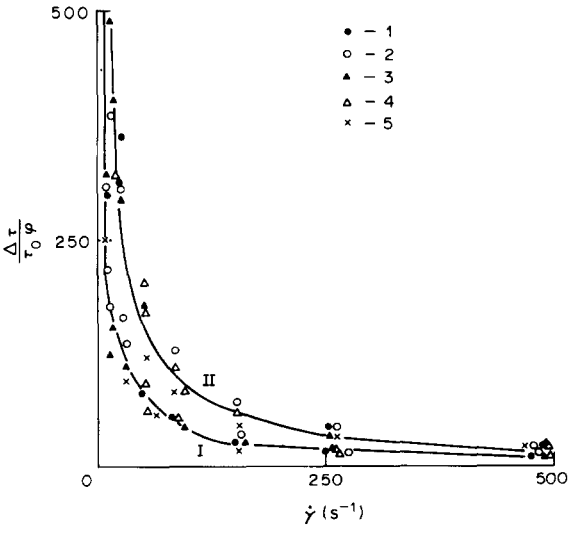

Figure 10. Relative shear stress increment vs shear rate, (I) $H = 24$ kA/m and (II) $H = 35,\ 3$ kA/m: 1, $\varphi = 0.02$; 2, $\varphi = 0.04$; 3, $\varphi = 0.06$; 4, $\varphi = 0.08$; 5, $\varphi = 0.1$.

strength and the concentration of the dispersed phase. In this case the dependence $\Delta\tau = \Delta\tau(\varphi)$ is close to the linear one within the entire concentration range (figure 9).

Relative variation of the shear stress increment, based on concentration, vs the shear rate for each field strength is generalized by one curve (figure 10). This linearity $\Delta\tau/\tau_{H=0}$ with respect to φ, i.e. independent of the characteristic viscosity $\eta_H - \eta_{H=0}/\eta_{H=0}\varphi$ of concentration, gives us grounds to think that the interaction effects of aggregates for the tested suspensions are absent or, at least, infinitesimal.

Thus, the following important facts have been found experimentally. An MRS is a suspension of non-interacting anisodiametric "loose" aggregates with a susceptibility of *ca.* 5, whose geometric parameters depend on a relationship between the magnetic and hydrodynamic forces.

4. MICROMECHANICS AND STRUCTURE OF MRSs

The experimental results produced allow an MRS to be described in terms of the static theory of flow of diluted suspensions of magnetic ellipsoidal particles in an external magnetic field (Pokrovsky 1978). The main aspects of the theory are as follows. Within the framework of hydrodynamics, consideration is given to inertialess Newtonian fluid flow around isolated non-deformable particles. A macroscopic stress tensor of suspensions is determined from volume- and direction-averaged macroscopic characteristics. Here, the contribution of individual particles is additive. An observed increase, as compared to the carrying medium, in apparent viscosity of such suspensions is due to energy dissipation when a solid phase is in the flow. Quantitatively this phenomenon is specified by the volumetric concentration of the particles and their form parameter $r_e = a/b$, where a is the semimajor axis and b the semiminor axis of an ellipsoid. If the particles are polarized (magnetized) and contained in an external field then their orientation relative to the flow may contribute greatly to an average stress. The most pronounced effect is achieved when long thin particles are oriented across the flow (Chaffey & Mason 1965; Pokrovsky 1978).

Based on these grounds and the experimental data obtained, the problem of the MRS description might be reduced to a trivial one if the MRS did not exhibit any principal difference from the traditional suspensions. In the case of MRSs we are concerned, not with rigid particles with fixed r_e but, with anisodiametric elements whose form parameter and orientation depend on the ratio of magnetic/hydrodynamic forces. In essence, the problem is reduced to searching for a dependence of r_e and an angle of orientation α of the major aggregate axis towards the flow orientation of such prescribed quantities as the external magnetic field strength, the concentration and magnetic properties of the dispersed phase, the continuous medium viscosity, the shear rate and other flow characteristics.

The following approach is suggested. From a balance of the hydrodynamic and magnetic torques affecting an aggregate in the shear flow a complex including all the prescribed parameters of the process is derived. Using the known formula of the theory of diluted suspensions, the characteristic viscosity as a function of this complex is found at different r_e. Since a continuous medium exhibits non-Newtonian properties in an MRS, a relevant description, in principle, should account for this. However, the theory of diluted suspensions with a non-Newtonian continuous medium is not sufficiently detailed to date. Hence, use is made of formulae for the Newtonian carrying medium but the complex "characteristic viscosity" includes apparent viscosity values at a given shear rate. This is permissible when the relative variation of the continuous fluid viscosity with shear rate along a particle is insignificant. Then the calculated characteristic viscosity values are compared to those experimentally obtained at the same S. The points of intersection of an experimental curve with a family of the calculated ones give r_e at the prescribed MRS deformation parameters. The angle of orientation α is found from a balance of the torques acting upon an aggregate and then a dynamic MRS microstructure is defined completely, whose parameters allow macroscopic relationships between magnetic susceptibility, rheological properties, heat and electric conduction to be found.

Now we analyse in detail the theoretical and experimental results by using the suggested approach. Consideration is given to the diluted suspension Couette flow of ellipsoidal aggregates not affected by external forces. The long axis of the aggregates is much smaller than the gap width (each aggregate may be considered as a single one in an infinite fluid). The aggregate on the side of the external magnetic field oriented across the flow is affected by a force moment. For this suspension a tensor of excessive stresses is of the form (Pokrovsky 1978):

$$\sigma = 2\eta_0\mathbb{D} + \eta_0\varphi_a[-\rho\langle\bar{\mathbf{e}}\cdot\mathbb{D}\bar{\mathbf{e}}\rangle\mathbb{E} + 2\alpha'\mathbb{D} + 2\beta D\times(3\langle\bar{\mathbf{e}}\otimes\bar{\mathbf{e}}\rangle - \mathbb{E}) + \epsilon(\langle\bar{\mathbf{e}}\otimes\mathbb{D}\bar{\mathbf{e}}\rangle + \langle\mathbb{D}\bar{\mathbf{e}}\otimes\bar{\mathbf{e}}\rangle) + \chi\langle\bar{\mathbf{e}}\otimes\bar{\mathbf{e}}\times(\bar{\mathbf{e}}\mathbb{D}\bar{\mathbf{e}})\rangle] - \tfrac{1}{2}N\lambda(\langle\bar{\mathbf{e}}\otimes\mathbb{L}\bar{\mathbf{e}}\rangle + \langle\mathbb{L}\bar{\mathbf{e}}\otimes\bar{\mathbf{e}}\rangle) - \tfrac{1}{2}N\langle\mathbb{L}\rangle; \quad [11]$$

where $\otimes$ is a dyad of vectors; $\bar{\mathbf{e}}$ is the unit vector of orientation of a symmetry axis of an ellipsoid; η_0 the continuous medium viscosity; $\mathbb{D}$ is the tensor of shear rates; $\mathbb{E}$ is the unit tensor; $\varphi_a = \varphi/\phi$ is the volumetric concentration of aggregates (φ is the volumetric concentration of the dispersed phase and ϕ is the degree of filling of the aggregate); N is the amount of particles per unit volume; $\mathbb{L}$ is the tensor of the moment of external forces; D is the rotational diffusivity; ρ, α', β, ϵ, χ and λ are the direction-averaged constants defined by the ellipsoid configuration (the values of these constants and D are given in appendix A). In sufficiently strong magnetic fields an ellipsoid is retained by the field from rotation and oriented at a fixed angle towards the flow. In this situation the moment of the magnetic forces $L_{x'}$ is equal to that of the hydrodynamic forces M_{hydr}. The latter is found from [11] as

$$M_{hydr} = \frac{16\pi}{3}\eta_0\dot{\gamma}ab^2\frac{r_e^2\sin^2\alpha + \cos^2\alpha}{A' + 2r_e^2(1-A')}, \quad [12]$$

where

$$A' = \frac{r_e}{r_e^2 - 1}\left(r_e + \frac{A_0}{2}\right);$$

A_0 is given in appendix A. The moment of the magnetic forces is

$$L_{x'} = \mu_0[M\times G], \quad [13]$$

where M is the magnetic moment of the ellipsoid and G is the effective magnetic field of the suspension. Using [4] we arrive at

$$L_{x'} = \tfrac{4}{3}\pi\mu_0\kappa_a ab^2 G_y G_z\left(\frac{1}{1+\kappa_a n_y} - \frac{1}{1+\kappa_a n_z}\right), \quad [14]$$

wherein G_y and G_z are determined by [7]. Equations [13] and [14] allow a functional relationship between the form parameter r_e, the angle α and the main characteristics of the process to be found:

$$\frac{r_e^2\sin^2\alpha + \cos^2\alpha}{2r_e^2(1-A') + A'}\frac{1}{G_z'G_y'}\frac{4}{\dfrac{1}{1+\kappa_a n_z} - \dfrac{1}{1+\kappa_a n_y}} - S = 0; \quad [15]$$

wherein

$$S = \frac{\mu_0\kappa_a H_e^2}{\eta_0\dot{\gamma}} \quad \text{and} \quad G_i' = |G_i|/H_e.$$

The complex S comprises all the given parameters of pure MRS shear flow in an external magnetic field and in the physical respect it represents a ratio of the characteristic magnetic and hydrodynamic moments of forces affecting the ellipsoid.

In the process scheme under consideration the assumption that the ellipsoids are fixed at a definite angle towards the flow is realized provided $S > S_{cr}$. This is related to a dependence of M_{hydr} and $L_{x'}$ on the angle of orientation α (figure 11). At fixed M_{hydr}, the

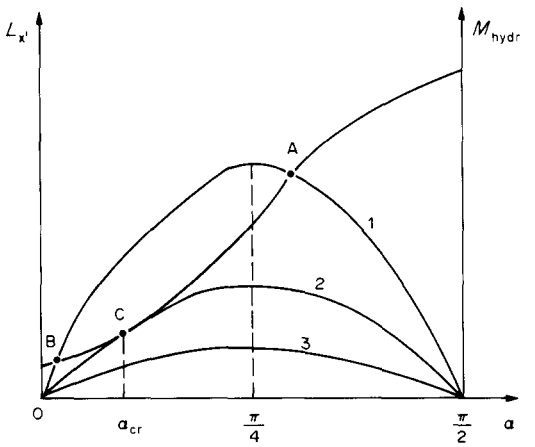

Figure 11. Magnetic ($L_{x'}$) and hydrodynamic (M_{hydr}) torques vs the angle of orientation.

situation is as follows. Depending upon the external magnetic field strength, the $L_{x'}$ curves may intersect that of M_{hydr} at two points (1), tough at one point (2) or have no common points (3). In the first case stable equilibrium of the ellipsoid is achieved only at point A. The second case is responsible for a minimum field which still prevents the ellipsoid from rotation. In this case the equilibrium angle is a minimum (point C) $\alpha = \alpha_{cr}$. In the third case the equilibrium is not attained and the ellipsoid is rotating in a shear flow. A relationship between α_{cr} and the prescribed parameters may be found from the solution of the following system of equations:

$$\left.\begin{aligned} M_{hydr}(\alpha, r_e, \eta_0 \cdot \dot{\gamma})|_{\alpha=\alpha_{cr}} &= L_{x'}(\alpha, r_e, \kappa_a \cdot H_e^2)|_{\alpha=\alpha_{cr}} \\ \left.\frac{dM_{hydr}}{d\alpha}\right|_{\alpha=\alpha_{cr}} &= \left.\frac{dL_{x'}}{d\alpha}\right|_{\alpha=\alpha_{cr}} \end{aligned}\right\} \quad [16]$$

This system is easily reduced to one equation which in an implicit form states the relationship between α_{cr} and r_e as

$$(r_e^2 - 1)(B_1 + B_2 \cos 2\alpha) \sin^2 2\alpha - 2(r_e^2 \sin^2\alpha + \cos^2\alpha)(B_2 + B_1 \cos 2\alpha + B_2 \sin^2\alpha) = 0;$$

$$B_1 = \tfrac{1}{2}(A_1A_3 + A_2A_4) \quad \text{and} \quad B_2 = \tfrac{1}{2}(A_2A_4 - A_1A_3). \quad [17]$$

The coefficients A_1, A_2, A_3 and A_4 are given by [8]. For the flow of suspensions of rigid polarizing particles in an external field the following conditions has been previously obtained:

$$\alpha_{cr} = \operatorname{arccot} r_e. \quad [18]$$

The solution of [18] does not satisfy [17]. This is due to the fact that a field in the suspension has been prescribed in the work by Shulman *et al.* (1977). In our case this is determined by the method of a self-consistent field and, therefore, it is a function of the angle of orientation of ellipsoids. Using a known value of α_{cr} from [15] we find S_{cr}.

For the Couette flow an expression for the characteristic viscosity follows from [11]:

$$[\eta] = \frac{\eta - \eta_0}{\eta_0 \varphi_a} = \frac{(\frac{3}{2}r_e^2 - r_e^2A' - \frac{5}{4}A')(r_e^2 - 1)}{(r_e^2 - \frac{3}{2}A')(2r_e^2 - 2r_e^2A' + A')} \sin^2 2\alpha$$

$$+ \frac{(2 - A')(r_e^2 - 1)}{(3A' - 2)(2r_e^2 - 2r_e^2A' + A')} \cos^2 2\alpha$$

$$- \frac{2(r_e^2 - 1)\cos 2\alpha}{2r_e^2 - 2r_e^2A' + A'} - \frac{r_e^2 + 1}{2r_e^2 - 2r_e^2A' + A'}. \quad [19]$$

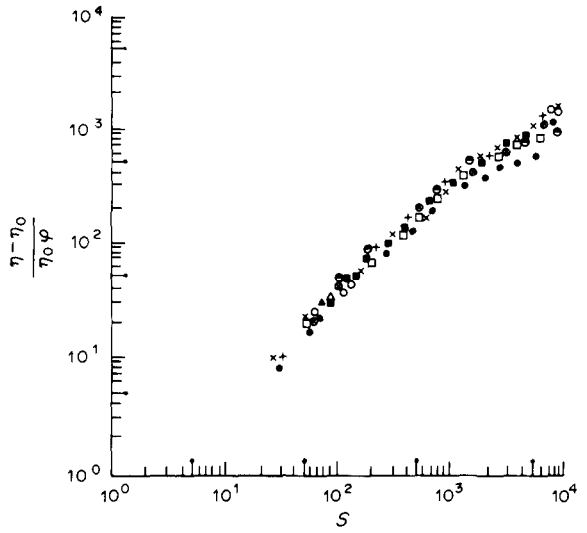

Figure 12. Characteristic viscosity vs the parameter S for $H = 24$ kA/m (points 1, 3, 5, 7, 9) and $H = 35.3$ kA/m (points 2, 4, 6, 8): ● ○, $\varphi = 0.02$; ▲ △, $\varphi = 0.04$; + ×, $\varphi = 0.06$; □ ■, $\varphi = 0.08$; ⊖ ⊗, $\varphi = 0.1$.

When deriving [19] account has been taken of

$$N = \frac{\varphi_a}{v}$$

($v = \frac{4}{3}\pi ab^2$ is the ellipsoid volume). The desired dependence $[\eta] = f(r_e, S)$ is obtained from [19] and [15] by eliminating $\alpha > \alpha_{cr}$.

The next step is the determination of $r_e = r_e(S)$. For this purpose the calculated characteristic viscosity values are compared with the experimental data produced for an increase in relative MRS viscosity in a magnetic field. Both in the calculations and experimentally we determine $\eta_H - \eta_{H=0}/\eta_{H=0}\varphi$, where η_H is the apparent viscosity of the suspension in the field while $\eta_{H=0}$ is the same outside the field. This enables one to take account of the effect of the rheological properties of the continuous medium. Normalization is performed with respect to the volumetric concentration of the dispersed phase but not with respect to the concentration of aggregates φ_a, since the former is prescribed in the experiments. Figure 12 shows the measured characteristic viscosity vs the variation of the prescribed parameter of the process, i.e. its dependence on S. Correlation of all the experimental points with a single curve confirms the validity of using S as a governing parameter. The points of intersection of the experimental curve $\eta_H - \eta_{H=0}/\eta_{H=0}\varphi = f(S)$ with those calculated for different r_e give $r_e = r_e(S)$ (figure 13). Here, the branching of the concentration curves is attributed, in the first instance, to the influence on the effective field

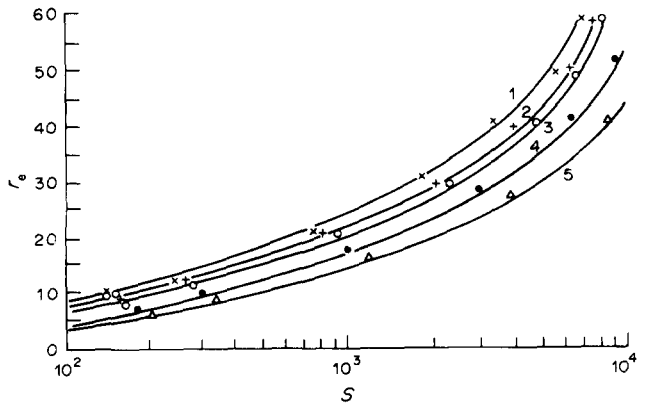

Figure 13. Parameter r_e vs complex S: 1, $\varphi = 0.02$; 2, $\varphi = 0.04$; 3, $\varphi = 0.06$; 4, $\varphi = 0.08$; 5, $\varphi = 0.1$.

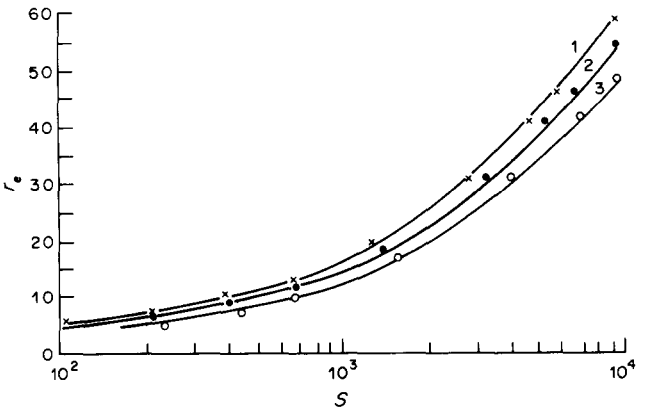

Figure 14. The effect of the extent of filling of the aggregate on $r_e = r_e(S)$: 1, $\varphi = 0.6$; 2, $\varphi = 0.5$; 3, $\varphi = 0.4$.

in the suspension. As follows from [7] an increase in the concentration results in a decrease in the effective field strength of the suspension. This decreases the magnetic torque and, therefore, r_e and α. The departure of real MRS structure from a theoretical scheme is inevitable. For instance, the influence of such a problematic factor as the extent of filling of an aggregate with particles ϕ is shown in figure 14. In the calculation of the present curves it has been taken as equal to 0.4, 0.5 and 0.6, respectively although r_e proved to be almost independent of ϕ, some branching of the curves took place and was comparable to that observed above. Henceforth, ϕ was taken equal to 0.5 and, respectively, $\kappa_a = 5$. Figure 15 shows the dependence of the angle of orientation α on S, found by the known r_e values. With an increase in S the aggregates turn in the field direction but only to some definite angle. With a further increase in S this angle practically remains the same and the apparent viscosity growth observed seems to be due only to an increase in r_e. This moment will be discussed in detail below. In addition to the data for the concentrations prescribed in the experiments, figure 15 displays the calculated dependence $\alpha = \alpha(S)$ for a very diluted suspension with $\varphi = 0.0001$. The dependence is in immediate proximity to the curve $\alpha = \alpha(S)$ for the MRS with $\varphi = 0.02$, i.e. the smallest-concentration system among those tested for which the condition prescribed by the theoretical model is fulfilled most completely. On the whole, the experimental and calculated data are in fair agreement. This conclusion is also verified by proper coincidence of the experimental dependences

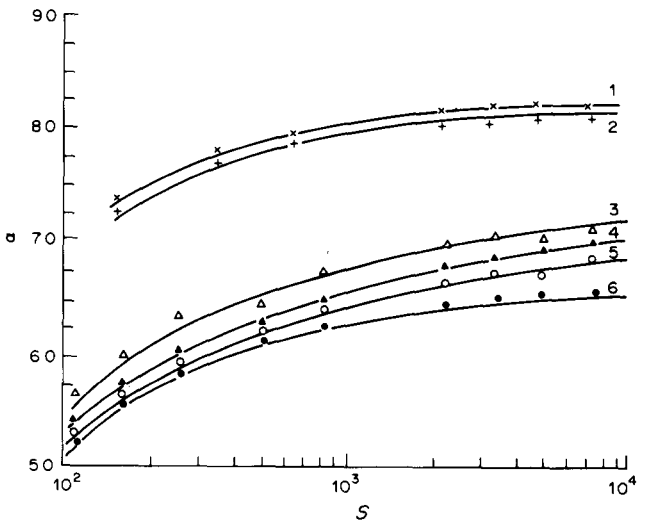

Figure 15. Angle of aggregate orientation vs S: 1, $\varphi = 0.02$; 2, $\varphi = 0.0001$; 3, $\varphi = 0.04$; 4, $\varphi = 0.06$; 5, $\varphi = 0.08$; 6, $\varphi = 0.1$.

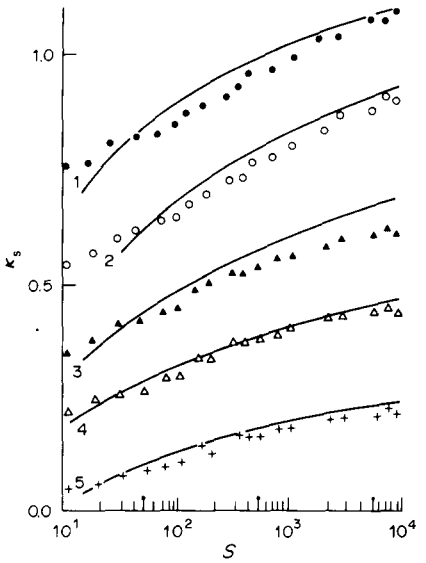

Figure 16. Magnetic susceptibility of the MRS vs S: 1, $\varphi = 0.1$; 2, $\varphi = 0.08$; 3, $\varphi = 0.06$; 4, $\varphi = 0.04$; 5, $\varphi = 0.02$. ——, Theory; ● ○ ▲ △ +, experimental.

$\kappa_s = \kappa_s(S)$ with those calculated by the relation $r_e = r_e(S)$, found from independent rheological measurements and by [5], [7] and [15] (figure 16).

Of some interest is the analysis of the mechanical behaviour of an MRS in a limiting case of large S, i.e. at great fields or small shear rates. When $r_e \gg 1$ but $2a$ is much less than the gap width, an expression for coefficient A' in [19] for the characteristic viscosity is reduced to the form

$$A' = 1 - \frac{\ln r_e}{r_e^2} \qquad [20]$$

and [19] is simplified and becomes

$$[\eta] \simeq \frac{2r_e^2}{\ln r_e}. \qquad [21]$$

An analogous limiting transition in [15] gives

$$S \simeq \frac{2r_e}{\ln r_e} \frac{1 + \kappa_a/2}{\alpha' \kappa_a/2}, \qquad [22]$$

where

$$\alpha' = \frac{\pi}{2} - \alpha.$$

From [21] and [22] it follows that

$$\frac{\eta - \eta_0}{\eta_0 \varphi} \simeq \alpha' \varphi_0 \frac{\kappa_a/2}{1 + \kappa_a/2} S. \qquad [23]$$

Multiplying term by term [23] by $\dot{\gamma}$ we arrive at the following rheological equation:

$$\tau = \eta_0 \dot{\gamma} + \alpha' S \eta \dot{\gamma} \varphi_a \frac{\frac{\kappa_\alpha}{2}}{1 + \frac{\kappa_\alpha}{2}}; \qquad [24]$$

or

$$\tau = \eta_0 \dot{\gamma} + \mu_0 H_e^2 \varphi_a \alpha' \frac{\kappa_a^2}{2 + \kappa_a}. \qquad [25]$$

As has been shown earlier, at great S the angle of orientation of the particles asymptotically approaches some constant value (figure 15). In this case [25] coincides formally with the Shvedov–Bingham equation, known in rheology for viscoplastic materials,

$$\tau = \eta\dot{\gamma} + \tau_0. \qquad [26]$$

However, in the physical sense, the second terms in [25] and [26] are quite different. In the first case one is concerned with the constants of mechanical energy dissipation over an aggregate (an increase in $\dot{\gamma}$ is followed by a corresponding decrease in r_e), while in the case of a conventional viscoplastic medium τ_0 indicates the limit of structure strength.

5. PROPERTIES OF THE STRUCTURAL ELEMENTS OF MRSs

The complex S, containing all the prescribed external parameters, as well as the relations obtained above, with the help of S, are valid only for shear flow. Their possible use in other types of flows, e.g. in extension flows, requires the additional description of the intrinsic aggregate properties of the flow, specifying its strength.

Thus, consider the forces affecting an ellipsoid in shear flow. The stresses over its surface in a system of coordinates related to it (figure 4) are written as (Jeffery 1922)

$$\sigma_y = -p_0 P\frac{y}{b^2} + \frac{8\eta_0 P}{abc}\left(G\frac{z}{a^2} + C\frac{y}{b^2}\right) - 4\eta_0 P(\alpha_0 A + \beta_0 B + \gamma_0 C)\frac{y}{b^2}$$

and [27]

$$\sigma_z = -p_0 P\frac{z}{a^2} + \frac{8\eta_0 P}{abc}\left(A\frac{z}{a^2} + G'\frac{y}{b^2}\right) - 4\eta_0 P(\alpha_0 A + \beta_0 B + \gamma_0 C)\frac{z}{a^2}$$

where P is the distance between a tangent at the point (y, z) and the origin of the coordinates,

$$P = \left(\frac{y^2}{b^4} + \frac{z^2}{a^4}\right)^{-1/2},$$

p_0 is the hydrostatic pressure and $b = c$, α_0, β_0 and γ_0 are the elliptic integrals in appendix A; A, B, C, G and G' are given in appendix B. For the most interesting case of large r_e (strong magnetic fields) the elliptic integrals allow a simple representation. Here the stresses are of the form

$$\sigma_y = -p_0 P\frac{y}{c^2} + \frac{8\eta_0 P}{ac^2}\left(\frac{\dot{\gamma}}{4}\frac{\cos 2\alpha' + 1}{2\ln r_e + 1}za - \frac{\dot{\gamma}}{24}\frac{\sin 2\alpha'}{2\ln r_e - 1}\frac{a^2}{c^2}ya\right) + \frac{\dot{\gamma}}{3}\eta_0 P\frac{\sin 2\alpha'}{2\ln r_e - 1}\frac{y}{c^2}.$$

and

$$\sigma_z = -p_0 P\frac{z}{a^2} + \frac{8\eta_0 P}{ac^2}\left(\frac{\dot{\gamma}}{12}\frac{\sin 2\alpha'}{2\ln r_e - 1}za + \frac{\dot{\gamma}}{4}\frac{2\ln r_e \cos 2\alpha' - 1}{2\ln r_e + 1}ya\right) + \frac{\dot{\gamma}}{3}\eta_0 P\frac{\sin 2\alpha'}{2\ln r_e - 1}\frac{z}{c^2}. \qquad [28]$$

Analysis of [28] shows that in the case under consideration ($r_e \gg 1$) the stress $\sigma = \sqrt{\sigma_y^2 + \sigma_z^2}$ attains its extreme value at the point $z = \bar{z}$, defined from the solution of the transcendental equation

$$[2BC\cos 2q - (A^2 + B^2 - C^2)\sin 2q](\cos^2 q + r_e^2 \sin^2 q) = r_e \sin 2q\,[(A^2 + B^2 - C^2)\cos^2 q + C^2 + BC\sin 2q], \qquad [29]$$

where

$$q = \arccos\bar{z}, \quad A = \frac{2\eta_0\dot{\gamma}P}{c^2}\frac{\cos 2\alpha' + 1}{\ln r_e + 1},$$

$$B = \frac{2}{3c^2}\eta_0\dot{\gamma}\frac{\sin 2\alpha'}{2\ln r_e - 1},$$

$$C = \frac{2\eta_0\dot{\gamma}P}{c^2}\frac{2\ln r_e \cos 2\alpha' - 1}{2\ln r_e + 1}$$

and

$$P = a[\bar{z}^2 + r_e^2(1 - \bar{z}^2)]^{-1/2}.$$

Solution of [29] for $\alpha^1 \sim 0.1$, $r_e \gg 1$, yields

$$\tilde{z} = \frac{a \cos \alpha' \ln r_e}{8r_e^3}.$$

Then

$$\sigma_{max} = \sigma|_{\bar{z}=a} \simeq \sigma_y|_{\bar{z}=a} \simeq 2\eta_0\dot{\gamma}\frac{r_e^2}{\ln r_e}. \quad [30]$$

Equation [30] determines the stress of aggregate poles resulting in a cut in "excessive" particles which are held by the magnetic forces acting between the particles. Now we shall try to define them. An interaction force between particles F_{magn} at a distance Δ from each other is related to the magnetic energy density w_{magn} by

$$F_{magn} = \frac{w_{magn}}{\Delta}.$$

The magnetic energy density inside an ellipsoid is $w_1 = B_a^2/2\mu_a\mu_0$ (μ_a is the magnetic permeability of the aggregate and B_a is the magnetic induction inside the aggregate). The energy per particle of radius R is

$$w = \frac{B_a^2}{\mu_0\mu_a}\frac{2\pi R^3}{3\phi}.$$

As a result we get

$$F_{magn} = \frac{B_a^2}{\mu_0\mu_a}\frac{2\pi R^2}{3\phi}\frac{R}{\Delta}. \quad [31]$$

The hydrodynamic "cutting" force per particle, according to [30], is

$$F_{hydr} = 2\pi R^2\dot{\gamma}\eta_0\frac{r_e^2}{\ln r_e}. \quad [32]$$

For sufficiently large r_e the demagnetizing factor along a major axis (according to [5]) is zero, hence $H_a = H_e$ and $B_a = \mu_0\mu_a H_e$. In the equilibrium state the following relation holds:

$$F_{hydr} = KF_{magn}. \quad [33]$$

Quantity K in [33] is an effective coefficient which depends on: (1) overestimation of the magnetic force defined by [31] which is valid only at $\Delta \ll R$; (2) underestimation of the hydrodynamic force because of the effective particle area in [32] being chosen as equal to πR^2; (3) the impossibility of the exact determination of the friction coefficient between the particles. From [31]–[33] we find

$$\frac{r_e^2}{\ln r_e}\frac{\eta_0\dot{\gamma}\,3\phi}{K\mu_0\mu_a H_e^2}\frac{\Delta}{R} \simeq 1. \quad [34]$$

Since

$$S = \frac{\mu_0\kappa_a H_e^2}{\eta_0\dot{\gamma}},$$

then [34] is equivalent to

$$\frac{r_e^2}{\ln r_e}\frac{1}{S} = K\frac{R(\kappa_a + 1)}{\Delta\kappa_a 3\phi} = \text{const}. \quad [35]$$

Relation [35] has been verified experimentally. Figure 17 displays

$$r_e^2 \ln r_e \frac{1}{S}$$

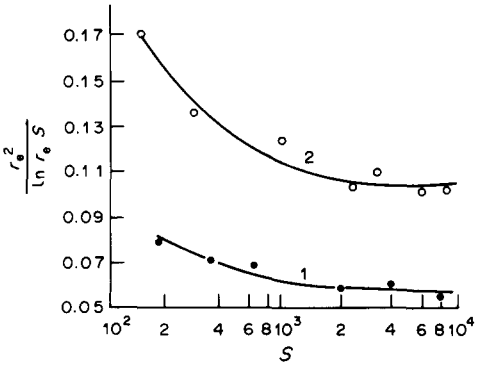

Figure 17. Plot of $r_e^2/\ln r_e S$ vs S: 1, $\varphi = 0.02$; 2, $\varphi = 0.1$.

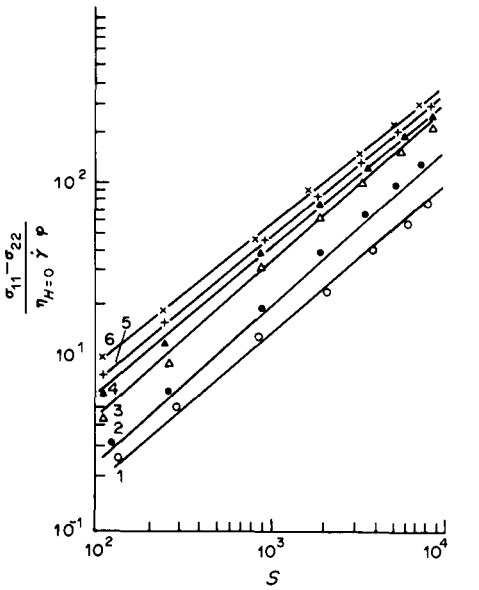

Figure 18. Reduced first difference of normal stresses vs complex S: 1, $\varphi = 0.0001$; 2, $\varphi = 0.02$; 3, $\varphi = 0.04$; 4, $\varphi = 0.06$; 5, $\varphi = 0.08$; 6, $\varphi = 0.1$.

as a function of S. Here use has been made of data from $r_e = r_e(S)$. As in seen from figure 17, at sufficiently large S, i.e. at $r_e \gg 1$ when [32] is valid, this complex is constant. On the other hand, [22] and [33] suggest that the angle between the long axis of the ellipsoid and the field direction is

$$\alpha' = K\frac{R}{\Delta}\frac{2(\kappa_a + 2)(\kappa_a + 1)}{3\phi\kappa_a}, \qquad [36]$$

i.e. it is constant at the prescribed MRS parameters. Besides, because of the small gap Δ between the particles the angle α' is small. Interpretation of the experimental data (figure 15) presented above has produced the same results. It allows theoretical estimation of the MRS structure parameters (r_e and α) for any type of flow differing from pure shear flow (for instance, for extension or at entrance regions). For this purpose it is sufficient to write a condition of equality of the moments of the forces acting upon the ellipsoid and that of the forces equality [33].

6. MACROSCOPIC RELATIONSHIPS

Detailed information on the structure allows determination of the whole series of physical properties of MRSs. Thus, having $r_e = r_e(S)$ and using [11] for the tensor of excess stresses one may obtain the dependences of all the rheological characteristics upon the complex S, namely:

(*a*) *the first difference of normal stresses* $(\sigma_{y'y'} - \sigma_{z'z'})$

$$\frac{\sigma_{y'y'} - \sigma_{z'z'}}{\varphi\eta_{H=0}\dot{\gamma}} = (\chi - 2\beta\lambda)\frac{\sin 4\alpha}{4} + \beta \sin 2\alpha; \qquad [37]$$

(*b*) *the second difference of normal stresses* $(\sigma_{z'z'} - \sigma_{x'x'})$

$$\frac{\sigma_{z'z'} - \sigma_{x'x'}}{\varphi\eta_{H=0}\dot{\gamma}} = \frac{\chi - 2\beta\lambda}{2}\sin 2\alpha \cos^2\alpha\left[\epsilon + \beta(\lambda - 1)\frac{\sin 2\alpha}{2}\right]; \qquad [38]$$

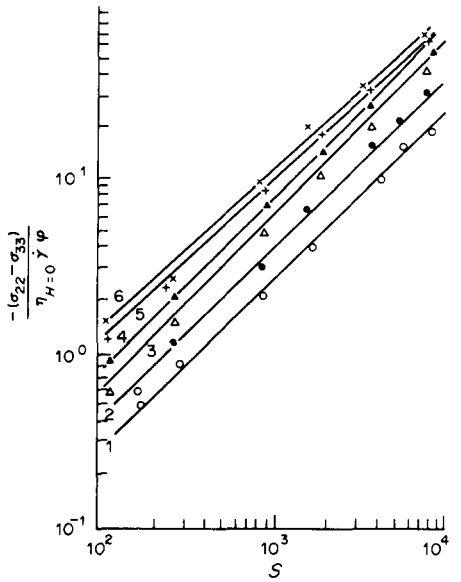

Figure 19. Reduced second difference of normal stresses vs complex S: 1, $\varphi = 0.0001$; 2, $\varphi = 0.02$; 3, $\varphi = 0.04$; 4, $\varphi = 0.06$; 5, $\varphi = 0.08$, 6, $\varphi = 0.1$.

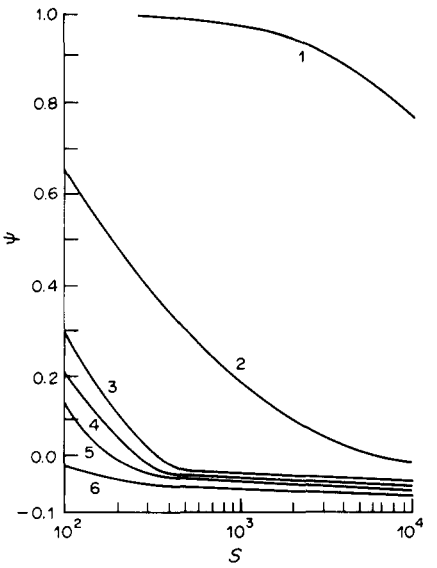

Figure 20. Degree of asymmetry of shear stresses vs S: 1, $\varphi = 0.0001$; 2, $\varphi = 0.02$; 3, $\varphi = 0.04$; 4, $\varphi = 0.06$; 5, $\varphi = 0.8$; 6, $\varphi = 0.1$.

(*c*) *a degree of asymmetry of shear stresses* ψ *which is attributable to superposition of the extremal moments* $\sigma_{y'z'} - \sigma_{z'y'} = L_{x'}$

$$\psi = \frac{\sigma_{z'y'}}{\sigma_{y'z'}} = \frac{1 + \varphi\left[\alpha + \frac{1}{2}(\epsilon + \beta\lambda - 3\delta) + \frac{1}{4}(\chi - 2\beta\lambda)\sin^2 2\alpha\right]}{1 + \varphi\left[\alpha + \frac{1}{2}(\epsilon + \beta\lambda + 3\delta) - \beta\cos 2\alpha + \frac{1}{4}(\chi - 2\beta\lambda)\sin^2 2\alpha\right]}, \quad [39]$$

where $\delta = \beta/3\lambda$.

The constants β, λ, χ, ϵ are listed in appendix A. The relation for mechanical energy dissipation as in the case of "symmetric" fluids is of the form

$$D = \sigma_{y'z'}\dot{\gamma}. \quad [40]$$

The influence of the complex S on the enumerated characteristics is presented in figures 18–20. It should be noted that at large values of S one may expect negative $\sigma_{z'y'}$.

6.1. Strength of the Structure Elements of MRSs

The case of the existence of small shear rates and large fields is possible when aggregates are so long that they overlap the entire flow section from the fixed wall to a movable one, thus forming peculiar bridges (figure 21). The movable wall entrains neighbouring particles while at the opposite end of the bridge they are held by the fixed wall. Thus, the bridge stretches and particles move away from each other. Because of the very small velocities, the hydrodynamic forces may be disregarded. The problem is reduced to the determination of the additional shear stress necessary to overcome the magnetic attraction of the forces. A similar problem for electrorheological suspensions has been considered previously by Shulman *et al.* (1977). In our case the attraction force for the particles amounts to

$$F = \frac{\pi\mu_f\mu_0\psi_m^2 R}{2\Delta(x)}, \quad [41]$$

where μ_f is the penetration factor of the dispersed medium, ψ_m the magnetic potential drop in the gap and $\Delta(x)$ is the distance between the particles. The additional impulse due to the bridge elongation is

$$P = \frac{1}{v}\int_0^{vT} F\sin\alpha\, dx, \quad [42]$$

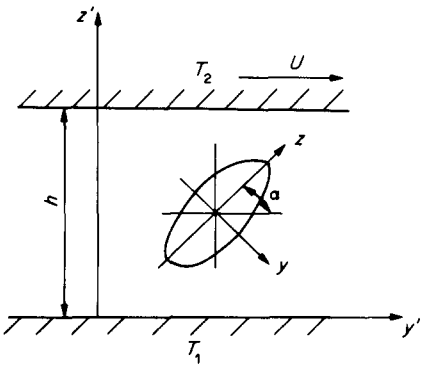

Figure 21. Calculation scheme.

where $T = \sqrt{5h/2v}$ is the lifetime of the bridge under the assumption that it breaks when particles move away from each other for a distance of the order of their radius, v is the velocity of the wall motion. Introducing N, the amount of bridges per unit area of the wall, we may determine the increment in shear stress due to elongation:

$$\Delta\tau = \frac{P \cdot N}{T}.$$

With regard to [41] and [42], and taking into consideration that

$$\Delta(x) = \Delta_{\min} + \frac{\sqrt{h^2 + x^2} - h}{n}$$

(n is the number of particles in the bridge and $\Delta_{\min}$ is the distance between the particles when the bridge is perpendicular to the plates), we derive

$$\Delta\tau = \frac{\pi\mu_0\mu_f\psi_m^2 R \cdot n}{\sqrt{5}} \frac{N}{h} 2I, \qquad [43]$$

where

$$I = \ln \frac{\frac{\sqrt{7}}{2} - a}{1 - a} \quad \left(a = 1 - \frac{\Delta_{\min} \cdot n}{h}\right),$$

herein $\Delta_{\min}$ is the initial distance between the particles. For the analysis of [43] it is more convenient to express N in terms of the volumetric fraction of the particles:

$$N \simeq \frac{3\varphi}{2\pi R^2}\left(n = \frac{h}{2R}\right).$$

Under the assumption that the gap between the particles is planar we find the drop in the magnetic potential to be

$$\psi_m \simeq \frac{H_e 2R}{1 + \frac{\mu_r \Delta_{\min}}{\mu_f 2R}}, \qquad [44]$$

where μ_r is the particle material permeability. As a result we arrive at the following expression for the increase in shear stress due to the elongation of bridges:

$$\Delta\tau = \frac{3I\varphi}{\sqrt{5}} \mu_0\mu_f H_e^2 \left(1 + \frac{\mu_f 2R}{\mu_r \Delta_{\min}}\right). \qquad [45]$$

The quantity $\Delta\tau$ determined by [45] for $\varphi = 0.1$, $H_e = 20$ kA/m, for carbonyl iron R-10-based MRS proved to be equal to *ca.* 60 N/m^2 and is in a fair agreement with the experimental results, $\Delta_{exp} = 50$ N/m^2 produced at shear rate $\dot{\gamma} = 0.3$ s^{-1}.

REFERENCES

ATABEKOV, G. I. 1969 *The Fundamentals of Circuit Theory*, p. 424. Energiya, Moscow.

BATCHELOR, G. K. 1976 Developments in microhydrodynamics. Theoretical and applied mechanics. *Proc. 14th IUTAM Congr.*, Delft, The Netherlands, pp. 136–187.

BIBIK, E. E. 1981 *Rheology of Dispersed Systems*, p. 171. Leningrad State Univ. Press, Leningrad.

CHAFFEY, C. E. & MASON, S. G. 1965 Particle behaviour in shear and electric fields: IV. The viscosity of suspensions of nonrotating ellipsoids. *J. Colloid Sci.* **20,** 330–340.

DUKHIN, S. S. & SHILOV, V. I. 1972 *Dielectric Phenomena and A Double Layer in Dispersed Systems in Polyelectrolytes*, p. 122. Naukova Dumka Izdaniya, Kiev.

HARVEY, E. N. 1953 Effect of magnetic fields on the rheology of ferromagnetic dispersions. *J. Colloid Sci.* **8,** 543–547.

JEFFERY, I. B. 1922 The motion of ellipsoidal particles immersed in a viscous fluid. *Proc. R. Soc.* 161–179.

LANDAU, L. D. & LIFSHITS, E. M. 1957 *Electrodynamics of Continua.* GITTL, Moscow.

POKROVSKY, V. N. 1978 *Statistical Mechanics of Diluted Suspensions*, p. 185. Nauka, Moscow.

SHULMAN, Z. P. & KORDONSKY, V. I. 1982 *The Magnetorheological Effect*, p. 184. Nauka i Tekhnika, Minsk.

SHULMAN, Z. P., KHUSID, B. M. & MATSEPURO, A. D. 1977 Structurization of electrorheological suspensions in an electric field. Quantitative estimates. *Izv. Akad. Nauk beloruss. SSR ser. fiz. mat. Nauk* **3,** 122–127.

TOLMASSKY, I. S. 1976 *Carbonyl Ferromagnetics*, p. 240. Izdaniya Metallurgiya, Moscow.

APPENDIX A

$$D = \frac{3T}{16\pi\eta_0}\frac{a^2\alpha_0 + b^2\beta_0}{a^2 + b^2},$$

$$\rho = \frac{1}{3ab^4\alpha_0'\beta_0''}[2(\alpha_0'' - \beta_0'') + 3ab^2(\alpha_0\alpha_0'' - \beta_0\beta_0'')],$$

$$\alpha = \frac{\alpha_0}{ab^4},$$

$$\epsilon = \frac{4}{(a^2 + b^2)ab^2\beta_0'} - \frac{2}{ab^4\alpha_0'},$$

$$\chi = \frac{2\alpha_0''}{ab^4\alpha_0'\beta_0''} - \frac{8}{ab^2(a^2 + b^2)\beta_0'} + \frac{2}{ab^4\alpha_0'}$$

and

$$\lambda = \frac{a^2 - b^2}{a^2 + b^2},$$

where T is the absolute temperature and α_0, α_0', α_0'', β_0, β_0' and β_0'' are the elliptical integrals which in the case of an axisymmetric ellipsoid are analytically presented as follows:

$$\alpha_0 = \int_0^\infty \frac{dx}{(a^2 + x)^{3/2}(b^2 + x)^2} = -\frac{1}{b^3(r_e^2 - 1)}\left(A_0 + \frac{2}{r_e}\right),$$

$$\gamma_0 = \beta_0 = \int_0^\infty \frac{dx}{(a^2 + x)^{1/2}(b^2 + x)^2} = \frac{1}{b^3(r_e^2 - 1)}\left(\frac{A_0}{2} + r_e\right),$$

$$\alpha_0' = \int_0^\infty \frac{dx}{(a^2 + x)^{1/2}(b^2 + x)^3} = \frac{r_e^4}{4a^3b^2(r_e^2 - 1)^2}\left(2r_e^2 - 5 - \frac{3A_0}{2r_e}\right),$$

$$\beta_0' = \int_0^\infty \frac{dx}{(a^2 + x)^{3/2}(b^2 + x)^2} = \frac{2r_e^2}{a^3b^2(r_e^2 - 1)^2}\left(1 + \frac{r_e^2}{2} + \frac{3r_eA_0}{4}\right),$$

$$\alpha_0'' = \int_0^\infty \frac{x\,dx}{(a^2+x)^{1/2}(b^2+x)^3} = \frac{2r_e^2}{ab^2(r_e^2-1)^2}\left(\frac{r_e^2}{4}+\frac{1}{8}+\frac{4r_e^2-1}{16r_e}A_0\right),$$

$$\beta_0'' = \int_0^\infty \frac{x\,dx}{(a^2+x)^{3/2}(b^2+x)^2} = \frac{2r_e^2}{ab^2(r_e^2-1)^2}\left(-\frac{3}{2}-\frac{2r_e^2+1}{4r_e}A_0\right)$$

and

$$A_0 = \frac{1}{(r_e^2-1)^{1/2}}\ln\frac{r_e-(r_e^2-1)^{1/2}}{r_e+(r_e^2-1)^{1/2}}.$$

APPENDIX B

$$A = \frac{1}{6}\frac{2\alpha_0''\tilde{a}-\beta_0''\tilde{b}-\gamma_0''\tilde{c}}{\beta_0''\gamma_0''+\gamma_0''\alpha_0''+\alpha_0''\beta_0''},$$

$$B = \frac{1}{6}\frac{2\beta_0''\tilde{b}-\gamma_0''\tilde{c}-\alpha_0''\tilde{a}}{\Delta},$$

$$C = \frac{1}{6}\frac{2\gamma_0''\tilde{c}-\alpha_0''\tilde{a}-\beta_0''\tilde{b}}{\Delta},$$

$$\Delta = \beta_0''\gamma_0''+\gamma_0''\alpha_0''+\alpha_0''\beta_0'',$$

$$G = \frac{\gamma_0\tilde{q}-a^2\beta_0'\eta}{2\beta_0'(c^2\gamma_0+a^2\alpha_0)}, \quad G' = \frac{\alpha_o\tilde{q}+c^2\beta_0'\eta}{2\beta_0'(c^2\gamma_0+a^2\alpha_0)},$$

$$\beta_0' = \gamma_0', \quad \beta_0'' = \gamma_0'', \quad \tilde{a} = \frac{\dot{\gamma}}{2}\sin 2\alpha, \quad \tilde{b} = 0, \quad \tilde{c} = -\frac{\dot{\gamma}}{2}\sin 2\alpha,$$

$$\tilde{q} = \frac{\dot{\gamma}}{2}\cos 2\alpha \quad \text{and} \quad \eta = -\frac{\dot{\gamma}}{2}.$$